A Novel Approach to the Restoration of AFM Images by Employing an Estimated Impulse Response for the AFM Calculated Using a Square Pillar Sample

Ahmed Ahtaiba, Munther Gdeisat, David Burton, Francis Lilley and Mark Murphy

Abstract — **The Atomic Force Microscope (AFM) is a very important instrument for use in nanotechnology and biology since it can be used to measure a wide variety of objects, such as nano-particles and cells, either in air or liquid. However, the images that are measured using AFM are distorted because of the influence of the tip geometry and the dynamic response of the instrument. This influence means that the images do not accurately represent the real shape of the measured particles or cells. Therefore, it is necessary to reconstruct the AFM tip shape. This paper proposes a new approach (impulse response technique) to reconstruct the AFM tip shape from a square pillar sample that is measured using AFM. Once the tip shape is known, a deconvolution process is carried out between the estimated tip shape and typical AFM 'distorted' images in order to reduce the distortion effects. The experimental results and the computer simulations validate the performance of the proposed approach, in which it illustrates that the AFM image accuracy has been significantly improved. The blind tip estimation approach is the industrial and research standard algorithm for the restoration of AFM images. We therefore also compare the proposed algorithm with the blind tip estimation algorithm, via the use of both computer simulations and real AFM images, and our algorithm gives enhanced results.**

Index Terms—**Atomic force microscope, AFM, image restoration, deconvolution, and image morphology.**

I. INTRODUCTION

THE Atomic Force Microscope is a very useful tool in the biomedical engineering [1] and microelectronics industrial [2] sectors. An AFM image is a distorted representation of the sample, due to the convolution effect which is produced by the finite size of the AFM tip and the dynamic response of the instrument. The image restoration problem has been studied by many researchers in terms of firstly determining the cantilever tip shape for the AFM and subsequently using it to restore the AFM images using some form of deconvolution algorithm.

Manuscript received March 6, 2011; revised March 29, 2011.

The authors are with The General Engineering Research Institute (GERI), Liverpool John Moores University, James Parsons Building, Byrom Street, Liverpool L3 3AF, UK. Corresponding author's email is m.a.gdeisat@ljmu.ac.uk.

This static formulation of the image restoration problem ignores other dynamic parameters that affect the image acquisition process in the AFM, such as the scanning speed, the response of the x, y and z piezo materials, and the bandwidth of the feedback loop system. As is well-known in digital image processing theory, the impulse response of a linear time invariant system "fully characterises" this system. This implies that our proposed algorithm's aim of finding an estimate of the impulse response of the AFM should inherently take all these parameters into consideration and should produce a better and more faithful image restoration algorithm than those that already exist in the literature.

The first essential step at the front-end of digital image processing systems is that of capturing digital images. Many distortions occur during the image acquisition process and these distortions should be eliminated, or alleviated, by using image restoration algorithms. Examples of systems where these distortions occur are in astronomical imaging using telescopes, in confocal microscopy, computed tomographic (CT) scanners and many other applications. These are similar research problems to that of the image restoration of AFM images [3]-[5].

In this paper we propose a new method (referred to here as the impulse response technique), which is suitable for estimating the AFM tip shape from the AFM image of the square pillar sample. Both computer simulation and experimental results were used for estimating the AFM tip shape. In both computer simulation and experimental results, a Lucy-Richardson deconvolution process was used between the estimated AFM tip shape and the AFM image in order to obtain a more accurate AFM image [6].

II. THE ALGORITHM

It is proposed here that the determination of the three-dimensional impulse response of the AFM could be performed by taking the following steps. A standard AFM calibration sample that contains a grid of square pillars, with dimensions that are accurately known *a priori* to their measurement, is first measured using contact mode AFM for a region of interest that encompasses a single raised square pillar. The height of the square pillar is 100 nanometers. The 3D topographical image that is produced by the AFM for the sample contains the square pillar's surface profile, however this is broadened due to the convolution process between the

ISBN: 978-988-19251-4-5
ISSN: 2078-0958 (Print); ISSN: 2078-0966 (Online)

cantilever tip and the square pillar sample. Digital image processing algorithms are then used to determine the exact location of the square pillar within the image. As its height is known *a priori*, those pixels that belong to the square are subsequently subtracted and are thus removed from the image, as follows. Firstly, the four sections that represent the impulse response of the AFM were numbered, as shown in Fig. 1(a). Then, sections 1 and 2 were translated towards each other. Next, sections 3 and 4 were also moved towards each other. Finally, we moved both sections 1, 2 and also sections 3, 4 simultaneously towards the centre of the square, as shown in Fig. 1(b). The resultant image can be considered to be a representation of the three-dimensional impulse response of the AFM.

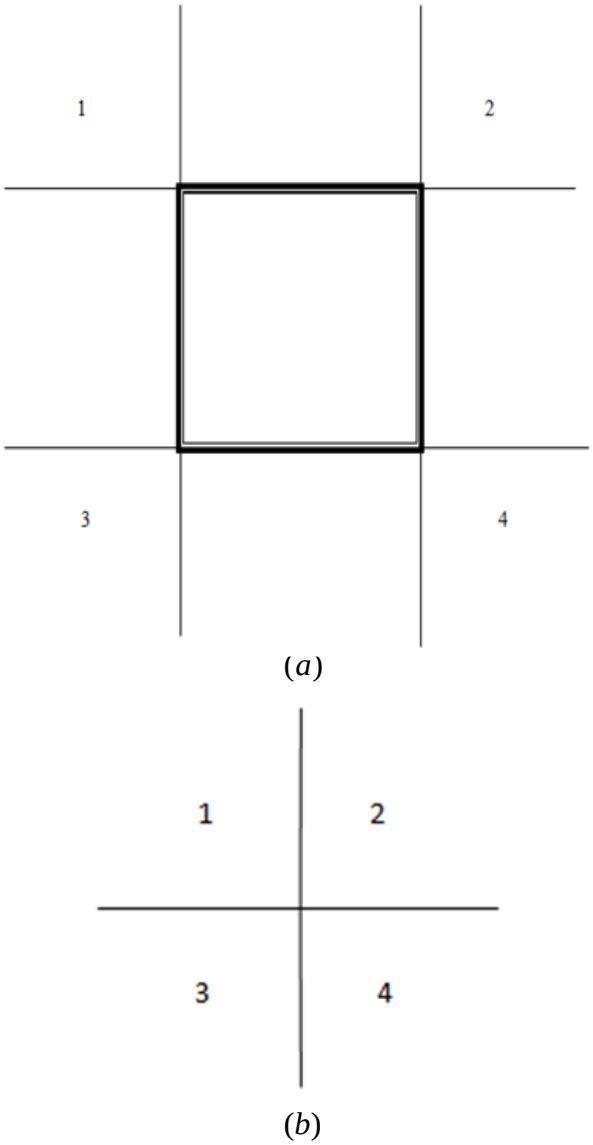

Fig. 1. Depicts the process of eliminating the square pillar from the image using the impulse response technique. (a) The selected four regions 1,2,3,4 that contain information about the AFM tip; (b) moving the four sections 1, 2, 3, 4 towards the middle of the central square. This results in eliminating those pixels that belong to the square pillar and the remaining result is an approximation of the impulse response of the AFM.

III. AFM TIP ESTIMATION

This paper presents a new technique for estimating the AFM tip shape from the square sample using a new impulse response method. The proposed approach uses a tip characterizer (square pillar sample) [7-9]. The AFM image of the square pillar sample is considered to be produced as a result of a convolution between the shape of the sample and the AFM tip. Thus, the AFM tip can be reconstructed by eliminating the effects of the tip characterizer topography from the AFM image of the square sample, at the same time taking into account dynamic effects. We have used a tip characterizer that consists of a standard square pillar sample and the impulse response approach for eliminating the effects of the tip characterizer geometry and dynamics from the AFM image. In this paper we will show that the proposed approach of using an impulse response method is effective for estimating 3-D tip geometry, which then can be used in the restoration of more accurate AFM images.

A. Computer Simulation

In the computer simulation, we have constructed computer models for both the AFM tip and the sample, in which the tip has a pyramidal shape and the sample has the shape of a raised square pillar, as depicted in Figs 2(a) and 2(b) respectively. An AFM image of the square pillar sample would be represented by a convolution process between the sample topography and the pyramidal tip. It is clear from Fig. 2(c) that after applying a convolution process between the simulated sample and simulated tip, the AFM image is now distorted by the AFM tip shape and no longer accurately represents the true sample topography. In order to improve the AFM image, it is therefore necessary to obtain information about the AFM tip shape. Once the tip shape is known, the reverse process of the convolution procedure (which is a deconvolution) can be applied between the distorted AFM image and the reconstructed tip shape in order to remove this distortion. The image of the simulated square pillar sample is then thresholded. The goal of this thresholding is to segment the grey level image into two regions, namely the background and the square pillar object itself. The optimal threshold value can be considered to be a grey level that separates an object region and a background region, without compromising the object's integrity [10].

Next, the outer boundary of the square pillar was determined using the edge Canny detection algorithm, which is well known as being an optimal edge detector. Once the outer boundary is detected, as illustrated in Fig 2(d), the pixels that belong to the image of the square pillar are eliminated. At the same time the data associated with the effects of the AFM tip, which are present around the outer perimeter of the eliminated square, are translated towards a position at the centre of the previously removed square. The resultant image, which is illustrated in Fig. 3, is an approximation of the impulse response of the AFM.

Any real experimental AFM topographic image may be regarded as being the result of the 'true' surface topography of the object that has been degraded by instrumental noise. Thus the AFM image can be represented as being a convolution of the actual topographic image $f(x,y)$ and a

ISBN: 978-988-19251-4-5
ISSN: 2078-0958 (Print); ISSN: 2078-0966 (Online)

degrading, or impulse response function, as in the following equation. Where x, y are the indices of pixels in the image.

$$g(x,y) = f(x,y) * I(x,y) + W(x,y) \quad (1)$$

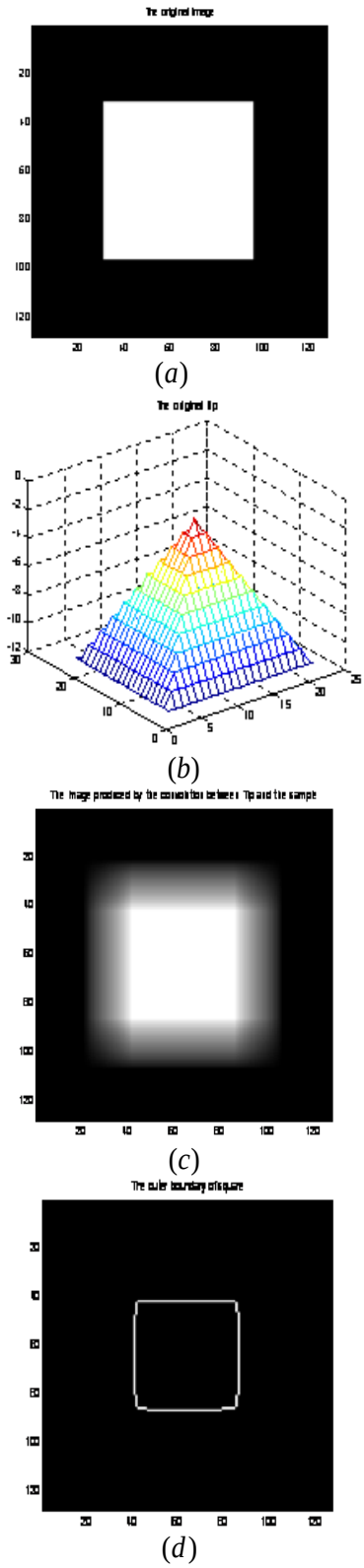

Fig. 2. Shows the simulation results for the impulse response technique using a square pillar sample. (a) the square pillar sample; (b) the AFM tip; (c) the image of the square sample that is produced by the convolution effect between the square pillar sample and the original AFM tip; (d) the outer boundary of the square pillar sample..

Where $g(x,y)$ is the degraded AFM image, $f(x,y)$ is the original 'true' sample topography, (*) indicates the 2D convolution effect between the sample and the tip, and $W(x,y)$ is a noise term.

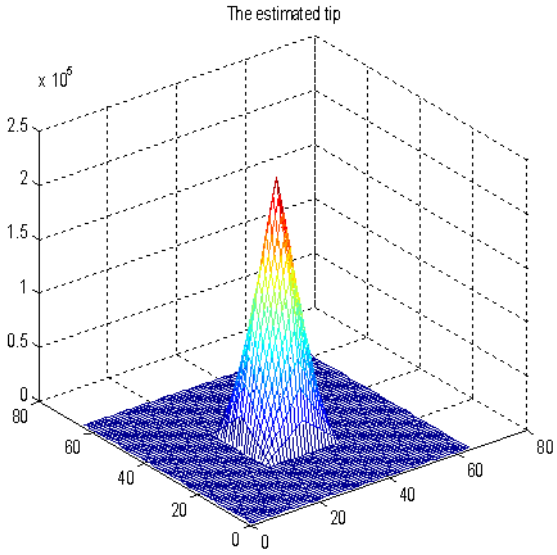

Fig. 3. Illustrates the simulation results showing the 3D image of the reconstructed tip shape.

Fig. 4(a) shows the two dimensional image of the square pillar sample that is analogous to a real AFM image, as it is a convolution between the pyramidal tip and the object's surface topography. Fig 4(b) shows the reconstructed image after applying a Lucy-Richardson deconvolution process between the reconstructed AFM tip shape and the blurred image of the square. The result of the deconvolution process, which comprises the reconstructed image, is slightly improved when compared with the original image.

B. Experimental results for estimating 3-D AFM tip shape

The three-dimensional impulse response of the AFM could be determined by performing the following steps. Measuring the topography of a standard AFM calibration sample using the AFM, as shown in Fig 5(a), that contains a raised square pillar with accurately known dimensions a priori to measurement. The 2-D topographical image produced by the AFM for the sample contains the square pillar's profile, but this is broadened due to the convolution effect between the 3D tip shape and the square pillar's true topography. Digital image processing techniques, such as thresholding and canny edge detection, were used to determine the exact location of the square in the image, as illustrated in Figs 5(b) and 5(c), respectively. As the height of the square is known *a priori*, the pixels that represent the square pillar may be eliminated by moving the inherent image distortions, that have been introduced due to convolution effects, to the centre of the image of the square. The resultant image may be considered to represent the three-dimensional AFM tip shape using the impulse response

ISBN: 978-988-19251-4-5
ISSN: 2078-0958 (Print); ISSN: 2078-0966 (Online)

method, and this is illustrated in Fig 5(d). Also, this image is considered to approximate the impulse response of the AFM.

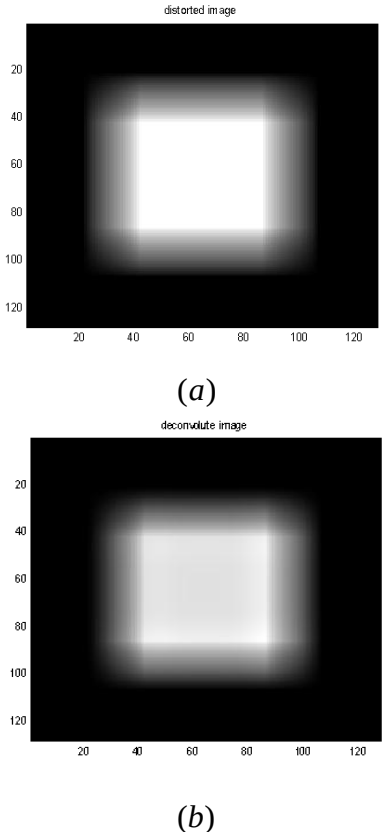

Fig. 4. Depicts simulation results for the impulse response technique. (a) The image of the sample due to the convolution between the square sample and the tip; (b) the image of the square sample after applying a Lucy-Richardson deconvolution.

IV. RESTORATION OF EXPERIMENTAL AFM IMAGES

Restoration of images that are subsequently produced by the AFM can be carried out by performing a deconvolution process between the raw AFM image that is acquired directly from the instrument and the approximated AFM impulse response that was described in the previous section. Many algorithms can be applied here to perform this task, such as the Wiener, Regularized filter, Lucy-Richardson, and Blind deconvolution algorithms [11].

The widely used Lucy-Richardson algorithm uses the *a priori* information of non-negativity and flux conservation. It produces a restored AFM image through an iterative method. The idea is to imagine that the ideal AFM image is convolved with the impulse response of the AFM. The Lucy-Richardson Algorithm maximizes the likelihood function of the image, which is modeled using Poisson statistics. The Lucy-Richardson algorithm uses such an iterative algorithm, as shown in (2).

$$f_{k+1}(x,y) = f_k(x,y)\frac{g(x,y)*h(-x,-y)}{[h(x,y)*f_k(x,y)]*h(-x,-y)} \qquad (2)$$

Where $h(-x,-y)$ is the transpose of the impulse response of the system, $f_k(x,y)$ is the previous estimate of the AFM image, $h(x,y)$ is the impulse response of the AFM system, and $f_{k+1}(x,y)$ is the current estimate of the AFM image.

The derivation and theory of operation of this algorithm has been described in detail in the original papers by Lucy [12] and Richardson [13].

Figs. 6(a) and 6(b) respectively, illustrate the simulations of the blurred AFM image and also the resultant restored AFM image that was produced by applying the deconvolution process. As a result of applying the deconvolution algorithm, it can be seen from Fig 6(b) that the quality of the restored AFM image has been improved by removing the effects of the AFM tip from the original blurred image.

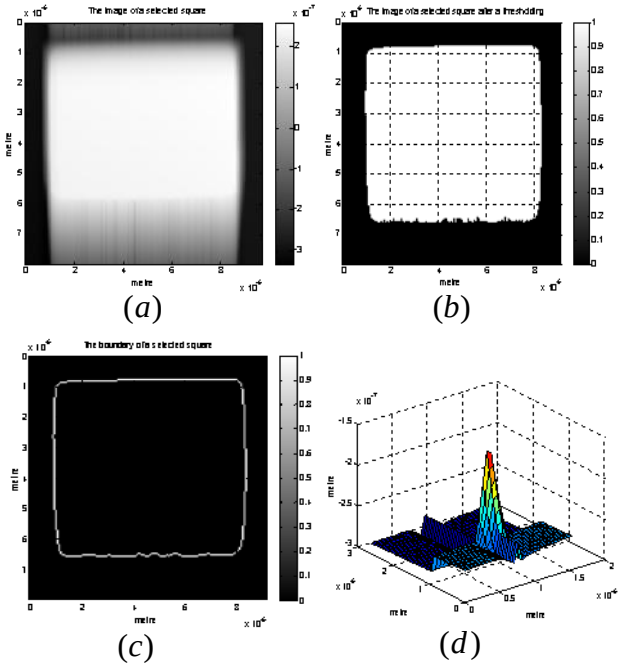

Fig. 5. Shows the experimental results for the impulse response technique, produced using a real AFM characterizer sample that contains raised square pillars. (a) The square pillar sample; (b) Thresholding a standard sample that contains a single square pillar with known dimensions; (c) Determining the location of the square pillar in the image by defining the outer boundary for removing the pixels that belong to the square pillar from the image; (d) Extracting the tip shape of the AFM.

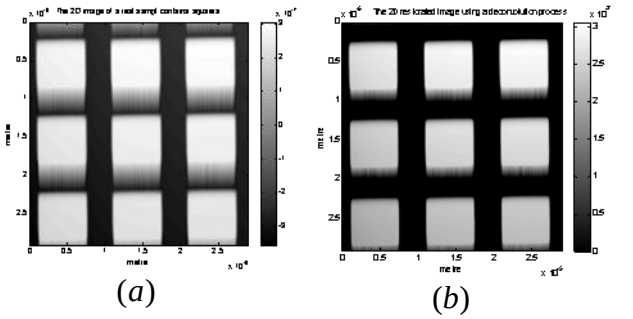

Fig. 6. Illustrates the experimental results for the impulse response technique using a Lucy-Richardson deconvolution algorithm for reconstructing a real AFM sample that contains raised square pillars. (a) The 2D image of a real sample that contains a grid of raised square pillars measured using AFM; (b) The 2D image of the same sample after applying a Lucy- Richardson deconvolution algorithm (the restored image).

ISBN: 978-988-19251-4-5
ISSN: 2078-0958 (Print); ISSN: 2078-0966 (Online)

Fig. 7 (a) shows an AFM topographical image of a single selected square pillar, produced by measuring a sub-region of the real sample that contains a grid of square pillars that was presented in Fig. 6. The restored AFM image after applying a Lucy-Richardson deconvolution algorithm is depicted in Fig. 7(b). As a result it can be seen that the level of distortion in the restored image has been reduced when compared with the original raw AFM image.

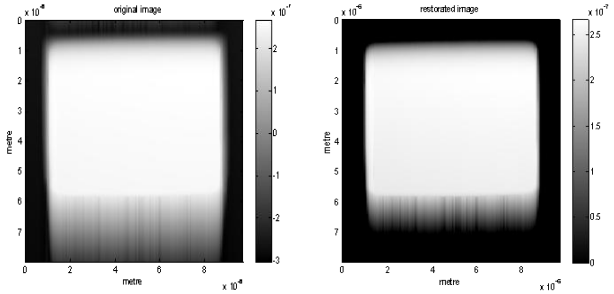

Fig. 7. Illustrates the experimental results for the impulse response technique using a Lucy-Richardson deconvolution method to restore the image of a real sample, consisting of a single raised square pillar. (a) The original image of the square pillar sample that was measured using the AFM; (b) the restored image of the square pillar sample after applying a Lucy-Richardson deconvolution algorithm.

V. BLIND TIP ESTIMATION ALGORITHM

Blind tip estimation algorithms rely on set theory and morphological operations [14], [15]. Here we introduce Villarrubia's method, which is based upon set theory. Using this technique, where the surface topography is unknown, it is possible to estimate the tip shape from the original AFM image of the sample. The image of the object is obtained by the dilation of the sample and the reflection of the tip P.

$$I = S \oplus P \tag{3}$$

Where I is the image of the sample, S is the genuine surface topography, and (P = -T) is the reflection of the tip T. In the case where the actual surface topography is known, then using erosion, the estimated tip topography is;

$$P_r = I \ominus S \tag{4}$$

Where P_r is the estimated 3D surface of the tip. Sample reconstruction by erosion can be written as;

$$S_r = I \ominus P \tag{5}$$

Where S_r is the reconstructed sample. The iterative process for blind tip estimation is defined by the following equation:

$$P_{i+1} = \bigcap_{\vec{x} \in I} [\,(I - \vec{x}) \oplus P'_i\,(x)] \cap P_i \tag{6}$$

In Equation (6), the calculation of the $(i+1)th$ iteration result is based on the $(i)th$ result. Where $\vec{x}$ is a point of interest in the image I.

$$P'_i(X) = (\vec{x} - I) \cap P_i \tag{7}$$

$P'_i(X)$ is a set of points in P_i that can contact the image I at a point of interest $\vec{x}$, with the apex point contained in the image I.

At convergence, the result of the estimated tip shape P_r can be determined as being;

$$P_r = \lim_{i \to \infty} P_i \tag{8}$$

Upon convergence, the final result gives the best estimate of the tip shape that has been obtained by blind reconstruction.

A. Experimental Results

A real sample that contains a grid of raised pillars was measured using an Asylum MFP-3D-IO AFM. The original image was captured by using contact mode AFM, where the tip scans across the sample surface. Fig. 8 shows the experimental results for the blind tip reconstruction algorithm. Fig. 8(a) illustrates the 3D reconstructed tip shape image. The original image of a real raised columnar grid sample that was measured by AFM is depicted in Fig. 8(b). This image has been created due to the dilation of the sample by the real AFM tip which was used to measure the sample. Finally an erosion operation by the estimated tip shape has been performed upon the original image (dilated image) in order to reconstruct the AFM image of the sample that is shown in Fig. 8(c). As a result, it can be seen that the restored image that was achieved as a result of the blind reconstruction approach is only slightly improved, when compared with the original image.

V. CONCLUSION

The impulse response technique using the square pillar sample has been demonstrated to be a useful tool in restoring AFM images. Both computer simulation and experimental results have shown improvements in the quality of AFM images after the application of the Lucy-Richardson deconvolution algorithm. Finally we have compared our algorithm with a standard existing approach to AFM image restoration that uses blind tip estimation and the results shown here indicate that application of the proposed algorithm leads to measurement results that are superior in quality to those that are produced by the blind tip estimation algorithm.

ISBN: 978-988-19251-4-5
ISSN: 2078-0958 (Print); ISSN: 2078-0966 (Online)

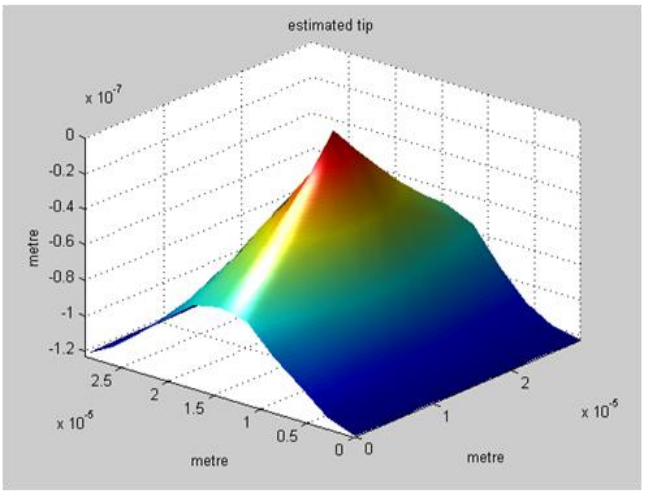

(*a*)

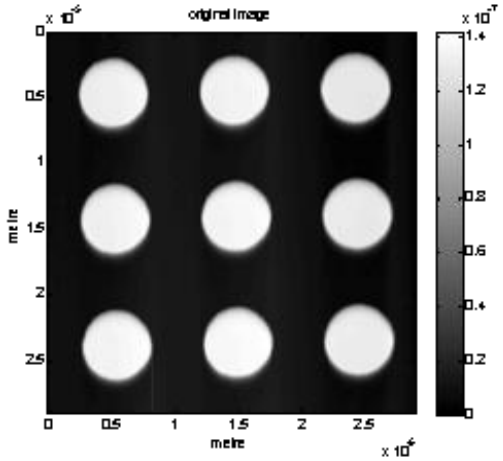

(*b*)

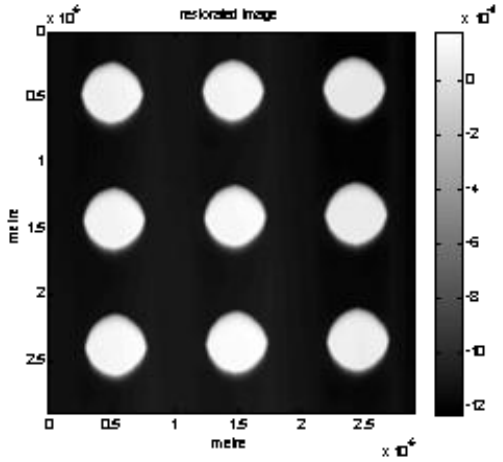

(*c*)

Fig. 8. Shows the experimental results of blind tip reconstruction using a real sample that contains a grid of cylindrical pillars. (a) The 3D image of the reconstructed tip using a blind tip estimation algorithm; (b) the 2D raw original AFM image of a real sample that contains cylindrical pillars; (c) the restored AFM image after applying the blind tip estimation algorithm.

REFERENCES

[1] K. Angelika, K. Christine, L. Alois, and B. Mizaikoff, " AFM - tip-integrated amperometric microbiosensors: high- resolution imaging of membrane transport", *Angewandte Chemie International Edition*, vol. 44, pp. 3419- 3422, 2005.

[2] J. Schneir, M. C. Sweenew, and T. H. Mcwaid," In fourth workshop on industrial applications of sccanning probe microscopy, NIST Gaithersbung, MD, USA, pp 30-31, 1997.

[3] M. Bertero and P. Boccacci, "Image restoration methods for the large binocular telescope", *Astronomy& Astrophysics Supplement Series*, vol. 147, No.2, pp. 323-333, 2000.

[4] P. J. Verveer, M. J. Gemkow and T. M. Jovin, "A comparison of image restoration approaches applied to three-dimensional confocal and wide-field fluorescence microscopy", *Journal of Microscopy*, vol. 193, No. 1, pp. 50-61, 1999.

[5] N. Nakamori, K. Tsukamoto and T. Tsunoo, "Image restoration of cone-beam CT images using wavelet transform", *Proceedings of The SPIE- The International Society for Optical Engineering*, vol. 3338, No.2, pp. 1275-1282, 1998.

[6] Gonzalez R., *Digital Image Processing*, Second Edition, Gatesmark publishing, 2008.

[7] H. Yasuhiko, S. Havato, H. Sumio, " Estimation of three dimensional Atomic Force Microscope tip shape from Atomic Force Microscope image for accurate measurement", *Japanese Journal of Applied phys.*, vol. 47, No. 7, pp. 6186-6189, 2008.

[8] N. Masao, N. Hideo, K. Kenji and M. Takahiro, " Critical dimension measurement in nanometer scale by using Scanning Probe Microscopy", *Japanese Journal of Applied physics*, vol. 35, pp. 4166-4177, 1996.

[9] N. Masao, N. Hideo, K. Kenji, I. Kazumi and M. Katsumi, " Metrology of Atomic Force Microscopy for Si nano- structures", *Japanese Journal of Applied physics*, vol. 34, pp. 3382-3387, 1995.

[10] T. Wenbing, J. Hai, Z. Yimin, L. Liman, and W. Desheng, *IEEE Transactions on systems*, vol. 38, No. 5, pp. 96-99, 2oo8.

[11] R. Gonzalez, *Digital image processing using matlab*, Second Edition, Gatemark Publishing, 2009.

[12] L. B. Lucy, "An iterative technique for the rectification of observed distributions", *The Astronomical Journal*, vol. 79, No.6, pp. 745-754, 1974.

[13] W. H. Richardson, "Bayesian- based iterative method of image restoration", *Journal of the optical society of America*, vol. 62, No.1, pp. 55-59, 1970.

[14] J. S. Villarrubia, "Algorithms for scanned probe microscope image simulation surface reconstruction and tip estimation", *Journal of Research of the National Institute of standards and Technology*, vol. 102, pp. 425- 454, 1997.

[15] T. Fenglei, Q. Xiaoping, and J. S. Villarrubia, " Blind estimation of general tip shape in AFM imaging", *Ultramicroscopy*, vol. 109, pp. 44-53, 2008.

ISBN: 978-988-19251-4-5
ISSN: 2078-0958 (Print); ISSN: 2078-0966 (Online)